Coevolution of retroviruses with *SERINC*s following whole-genome duplication divergence

Pavitra Ramdas[1], Vipin Bhardwaj[1], Aman Singh[1], Nagarjun Vijay[2], Ajit Chande[1*]

[1]Molecular Virology Laboratory & [2]Computational Evolutionary Genomics Lab from the Department of Biological Sciences, Indian Institute of Science Education and Research (IISER) Bhopal, India.

Abstract

The *SERINC* gene family comprises of five paralogs in humans of which *SERINC3* and *SERINC5* restrict HIV-1 in a Nef-dependent manner. The origin of this anti-retroviral activity, its prevalence among the remaining human paralogs, and its ability to target retroviruses remain largely unknown. Here we show that despite their early divergence, the anti-retroviral activity is functionally conserved among four human *SERINC* paralogs with *SERINC*2 being an exception. The lack of activity in human *SERINC*2 is associated with its post-whole genome duplication (WGD) divergence, as evidenced by the ability of pre-WGD orthologs from yeast, fly, and a post-WGD-proximate *SERINC*2 from coelacanth to inhibit HIV-1. Intriguingly, potent retroviral factors from HIV-1 and MLV are not able to relieve the *SERINC*2-mediated particle infectivity inhibition, indicating that such activity was directed towards other retroviruses that are found in coelacanth (like foamy viruses). However, foamy-derived vectors are intrinsically resistant to the action of *SERINC*2 and this resistance is conferred by a foamy virus envelope. Despite the presence of weak arms-race signatures, the functional reciprocal adaptation among *SERINC*2 and *SERINC*5 and, in response, the emergence of antagonizing ability in foamy virus appears to have resulted from a long-term conflict with the host.

Keywords: arms-race, *SERINC*, restriction factors, anti-retroviral, whole-genome duplication

Introduction

Viruses have been exploiting the host machinery for their persistence, and, in response, the host has continued to evolve increasingly intricate antiviral defense strategies. As part of this ongoing arms-race, while viruses have relied on acquisition and fusion of diverse genes (1), the host-defense mechanism has been made possible by the functional divergence of gene copies following duplication of genes as well as whole-genomes (2–7). Restriction factors being at the forefront of this long-term conflict (8–10), show clear molecular signatures of arms-race (11,12). In fact, the presence of these signatures has been proposed to be a hallmark of restriction factors (8,13), and has been used as a screening strategy to identify potential candidates(2,14). In contrast, the recently identified anti-retroviral host inhibitors *SERINC*5 and *SERINC*3 display an uneventful evolutionary history (15). This is counterintuitive, because distant retroviruses, with wide host-range, encode anti-*SERINC*5 virulent factors (16–18). We therefore sought to trace the origins of this antiretroviral activity and its relevance for retroviral

41 inhibition. Our analysis to comprehend the evolutionary origins of the antiretroviral activity in
42 *SERINC*s, identifies an active *SERINC*2 with a hitherto unknown interaction with a foamy virus.
43
44 **Results**
45 **Antiretroviral activity among human *SERINC* paralogs**
46 Analysis of sequence similarity and gene structure conservation reveals that *SERINC*5 and
47 *SERINC*4 share a recent ancestry **(Fig-S1)**. Similarly, *SERINC*3 and *SERINC*1 paralogs are
48 most similar to each other (~60% identity). Despite having the lowest sequence similarity to
49 either of the established anti-viral *SERINC* paralogs, *SERINC*2 is relatively similar to *SERINC*3
50 (50%) and *SERINC*5 (37%). Given such levels of sequence similarity and conserved membrane
51 topology **(Fig-S2)**, we checked the activity of other paralogs to inhibit HIV-1 infectivity in addition
52 to *SERINC*5 and *SERINC*3. From the native versions of *SERINC*1 and *SERINC*4 we failed to
53 express the proteins, so we decided to generate codon-optimized versions of these genes.
54 Having found the proteins being expressed upon codon optimization (**Fig1A**), we used these
55 conditions to check the inhibitory activity of all *SERINC* paralogs. We find that *SERINC*2 is the
56 only *SERINC* to have no activity against HIV-1 while all the other *SERINC*s inhibit the virus
57 infectivity to a varying degree (**Fig-1A and 1B**). Despite less-prominent membrane localization,
58 *SERINC*4 has a potent activity and is second-most powerful in inhibiting the virus (**Fig-1C**).
59 In contrast to other restriction factors, *SERINC*5 and *SERINC*3 genes have a rather uneventful
60 history that is distinct from the traditional signatures of recurrent selection seen in genes that
61 are part of an arms-race (19). We investigated the generality of whether the absence of
62 signatures of positive selection was prevalent across all the *SERINC* paralogs. Towards this,
63 we compared the evolutionary signature of *SERINC* genes with previously identified restriction
64 factors, genes showing recurrent positive selection and a few functionally characterized genes
65 that can act as controls **(Fig-1D)**. Within *SERINC* paralogs there is heterogeneity in the patterns
66 of positive selection, with *SERINC*1 and *SERINC*5 showing the least number of positively
67 selected residues while, *SERINC*3 and *SERINC*4 have relatively a greater number of residues
68 under episodic diversifying selection **(Fig-1D; FigS3, S4;** arms-race signature inference is
69 found to be sensitive to the multiple sequence alignment tool used, see **Fig-S5)**. Functionally
70 though, *SERINC*4 and *SERINC*5 are the most potent antiretroviral inhibitors compared to the
71 other three *SERINC*s, suggesting that merely the fraction of sites that are positively selected is
72 not an indicator of its ability to inhibit the retrovirus. Although the arms race signatures of few
73 restriction factors such as BST-2 and EIAF2AK2 were well correlated, the other newly identified
74 restriction factors including *SERINC*s did not show any consistent pattern of clustering **(Fig-**
75 **1D)**. One of the prime features of restriction factors has been their ability to get augmented
76 upon interferon stimulation. While the genes which formed a cluster are interferon responsive
77 (IFN responsive genes were obtained from ref (20)), this property did not explain the overall
78 pattern of clustering **(Fig-1D)**. Arms race signatures are not prominent in several interferon-
79 inducible genes and innate immune genes including TLRs **(Fig-1D)**. Hence the lack of arms
80 race signatures in *SERINC*s is probably not very surprising. The ability to restrict HIV-1 among

81 human *SERINC*1 and *SERINC*4 suggests that this is an evolutionarily conserved feature
82 despite the early divergence of these paralogous copies. Hence, we further decided to
83 investigate the evolutionary origins of this anti-retroviral activity.
84
85 **Anti-retroviral activity in an ancient feature among *SERINC*5 orthologs**
86 *SERINC*s plausibly shaped retroviral evolution, as indicated by the convergent emergence of
87 anti-*SERINC*5 activity among diverse retroviral genomes. *SERINC* gene family of restriction
88 factors is conserved across eukaryotic species with evident topological similarity **(Fig-S6)**, so
89 we asked to what extent the ability of *SERINC* orthologs to restrict HIV-1 is conserved.
90 Unicellular eukaryotes and invertebrates have a single copy of the *SERINC* gene (*TMS*1); all
91 these orthologs could restrict *nef*-defective HIV-1 (**Fig-1E and 1F**), albeit the yeast ortholog
92 having modest activity (2-fold) in comparison to all other orthologs (fold inhibition from 4-36).
93 This lower potency compared to all other orthologs could be attributed to inadequate
94 localization on the membrane or heterologous host expression for yeast and fly *TMS*1 in
95 conditions where the remaining orthologs were adequately expressed on the membrane (**Fig-**
96 **1G**). Western blot analysis confirmed the expression of C-terminal HA-tagged TMS-1 and other
97 *SERINC*5 orthologs (**Fig-1E,** lower panel).
98
99 **Coelacanth *SERINC*2 restricts HIV-1**
100 Two rounds of WGD in the ancestor of chordates led to a large increase in the number of genes
101 leading to the acquisition of new functions. This repertoire of genes also provides greater
102 flexibility due to their mutually compensatory functions. Hence post-WGD paralogous copies
103 tend to diversify. A single copy of *SERINC* gene (*TMS*1) is present in pre-WGD species and,
104 post- WGD, the number of copies has increased to five in tetrapods and six in bony fishes
105 **(FigS1)**. Our investigation of the pre-WGD ortholog of *SERINC* genes from the yeast (*S.*
106 *cerevisiae*) and the fly (*D. melanogaster*) *TMS1,* found evidence of anti-retroviral activity (**Fig-**
107 **1E**). Functional data on the human paralogs also suggests an ancestrally conserved activity of
108 *SERINC*s in restricting HIV-1, *SERINC*2, however, being an exception (**Fig1A**). Hence, the
109 human *SERINC2* paralog may have lost the ability to restrict HIV sometime after the WGD
110 (~700 to 400 MYA)(21). It is plausible that the species proximal to the WGD-event might retain
111 a version of *SERINC2* with antiviral activity **(Fig-2A)**. We, therefore, decided to systematically
112 screen *SERINC2* orthologs from post-WGD species at varying levels of sequence divergence
113 from human *SERINC2*. This exercise revealed that Coelacanth *SERINC*2 restricts HIV-1 in
114 conditions where *SERINC*2 isoforms from human did not show any activity (**Fig-2B**). A shorter
115 isoform of the Human *SERINC*2 (Human-201) was found to be topologically similar (**Fig-S7**) to
116 that of Coelacanth *SERINC*2 but lacked the activity to restrict HIV-1 concurrent with the longer
117 isoform.
118
119
120

121 **The gradual loss of antiretroviral activity in *SERINC2***

122 Upon further assessment of anti-HIV-1 activity of post-WGD *SERINC*2 orthologs, we find that
123 while Coelacanth *SERINC*2 reduced the infectivity by ~7-fold, Xenopus *SERINC*2 exhibited a
124 modest inhibition (~2-fold). The activity was completely lost in chicken *SERINC*2 ortholog
125 onwards, this is despite the topology being conserved and the levels of virus-incorporation for
126 chicken ortholog were also appreciable **(Fig-2C, S8 and S9)**. This lack of activity, however, is
127 persistent in mouse, horse and human *SERINC*2 **(Fig-2C and 2D)**. Coelacanth *SERINC*2
128 restricted HIV-1 to a lesser extent compared to human *SERINC*5; however, it was more potent
129 than human *SERINC*3 and *SERINC*1. Further, reduced restriction potency can be attributed to
130 its inadequate membrane presence **(Fig-2E)**, reminiscent of localization of the pre-WGD
131 orthologs from yeast and fly TMS-1 **(Fig-1G)**. We see that there is a dose-dependent inhibition
132 when coelacanth *SERINC*2 was expressed from the plasmids carrying the promoters of
133 different strengths (**Fig-S10**). Western blot of C-terminal HA-tagged *SERINC* expressors
134 verified that each of these *SERINC*2 orthologs is expressed from the synthetic genes **(Fig-2C,**
135 lower panel**)**. Loss of human *SERINC*2 antiviral activity could have been associated with
136 changes in pathogen repertoire or simply gain of a new function. To experimentally test if this
137 was in response to change in the pathogen repertoire, we asked if the counteraction of Human
138 *SERINC*5 by known retroviral factors, HIV-1 Nef[1] and MLV GlycoGag[1], was analogous to that
139 of Coelacanth *SERINC*2. In conditions where Nef and GlycoMA efficiently counteracted the
140 potent restriction imposed by Human *SERINC*5 and the partial restriction of Xenopus *SERINC*2,
141 we find that counteraction of Coelacanth *SERINC*2 restriction by these virulent factors was not
142 appreciable **(Fig-3A and 3B).** We also inspected if the nef alleles from human and non-human
143 primate lentiviruses showed a similar phenotype and found that nef alleles did not rescue the
144 infectivity comparable to that of *SERINC*5 **(Fig-3C)**. This is in conditions where the activity of
145 coelacanth *SERINC*2 also phenocopied to that of human *SERINC*5 in terms of the envelope
146 sensitivity **(Fig-3D)** indicative of an analogous action. However, the retroviral factors still failed
147 to rescue the inhibition.

148

149 **Functional evidence for arms-race dynamics**

150 Is this another functional evidence for arms-race dynamics as three distinct genera of
151 retroviruses are reported to have independently come up with antagonizing factors **?**(16–18,22)
152 **(Fig-3E)**. We learnt that coelacanth fish has an endogenous foamy virus (23) the genome
153 organization of which resembled the prototype foamy virus (**Fig-4A**). The activity of coelacanth
154 *SERINC*2 may have been linked to a foamy virus infection of the host. To experimentally test
155 the idea of whether *SERINC*2 has in-fact evolved to restrict foamy viruses, we checked the
156 presence of anti-foamy virus activity in human *SERINC* paralogs as well as the *SERINC*2
157 orthologs. Unexpectedly, we find that foamy is insensitive to any of the human *SERINC*
158 paralogs tested as well as the coelacanth *SERINC*2, in conditions where HIV-1 was consistently
159 inhibited **(Fig-4B)**. We argued that this might have been associated with an intrinsic ability of a
160 Foamy virus-encoded factor to counter the inhibition. To dissect this, we co-expressed foamy

genes individually to check its ability to rescue, now, *nef*-defective HIV-1 such that the insensitivity of foamy and the presence of antagonizing factor can be revealed. Surprisingly, with none of the foamy components expressed in-*trans* we find an ability to rescue the *nef*-defective HIV-1 in the presence of Human *SERINC*5 **(Fig-4C)**. The inhibition exerted by coelacanth *SERINC*2, however, was antagonized by the Envelope glycoprotein of Foamy virus using an equivalent amount of nef expressing plasmid **(Fig-4D),** as well as in a dose-dependent manner **(Fig-S11)**. We interrogated if this rescue was an effect of cross-packaging of the HIV-1 core by the foamy-virus envelope glycoprotein. By using a pseudoparticle comprising of an HIV core complemented with the foamy-virus envelope, we show that this was not an effect of cross packaging **(Fig-S12),** and that this rescue by the envelope glycoprotein was specific to its ability to antagonize coelacanth *SERINC*2 **(Fig-4D)**. To then understand the specificity of this counteraction, we checked the expression of Coelacanth *SERINC*2 at protein level when co-expressed with Foamy envelope. We checked the effect with both low expression (PBJ6) and high expression(pcDNA) of Coelacanth SERINC2 and observed that the steady state levels of Coelacanth SERINC2 is affected in the producer cells when Foamy envelope was co-expressed **(Fig-4E)**. Further, we questioned as to whether the foamy virus was at all sensitive to the effects of coelacanth *SERINC*2. To answer this, we pseudotyped a foamy-virus core, now, with an envelope glycoprotein of HIV-1 lacking a c-terminal domain, for packaging of a heterologous foamy core since the native, full-length, envelope glycoprotein of HIV-1 was not capable of the packaging it **(Fig 4F)**. After successful packaging, we show that intrinsically the foamy core is sensitive **(Fig 4F)**. This advocates that foamy-virus is indeed sensitive to coelacanth *SERINC*2 and has developed a mechanism to antagonize the inhibitory effect through the envelope glycoprotein likely as part of an ongoing arms-race.

Discussion

The use of comparative evolutionary genetic approaches has continued to enrich our understanding of restriction factor biology for more than a decade(24–28). Reciprocal loss of duplicated genes in different species has been shown to contribute to species-specific differences in susceptibility to pathogens(29–32). Similar to reciprocal gene loss, we find that *SERINC*2 and *SERINC*5 show reciprocal functional adaptation against divergent retroviruses. The ability of these orthologous factors to restrict HIV-1 is remarkable, even in the heterologous hosts **(Fig1E, 2C and Fig-S13)** suggestive of a topology associated feature that remained conserved and contribute to virus restriction. Further, the *SERINC*s from a human can restrict divergent viruses, like MLV(16,17), EIAV(15,18), this only indicates a long-term interaction of these host factors which exerted a strong selective pressure in order to shape their evolution.

Exogenous retroviruses have not yet been reported from pre-WGD species that we considered here so the range of targets that a pre-WGD *SERINC* (TMS-1) still remains to be identified. The restriction on mobility of genetic elements in yeast has earlier been shown conserved in APOBEC. While genes such as CCR4 and DHH1 that physically interact with TMS-1 have been implicated in yeast retrotransposon activity (33,34) the mechanism that TMS-1 would manifest

201 on retroelements remains to be investigated. TMS-1 in fly may still be required to regulate the
202 mobility of gypsy retroelements as the gypsy envelope has been shown to pseudotype MoMLV-
203 based vector to efficiently infect fly cells (35,36). Moreover, the analogous mechanism that
204 Rous sarcoma virus uses to produce Pr180gag-pol has been found in yeast Ty-1 transposons
205 (37), makes such existence of retroelement interactions for other host-factors like TMS-1 more
206 probable. Post-WGD, *SERINC* has five copies and this may have been associated with tackling
207 increasing diversity of pathogens during speciation and while doing so retaining its core
208 function. As demonstrated here, with cross-packaging studies we show that *SERINC*2 ortholog,
209 which was thought to be inactive, may potentially have constituted a critical barrier to foamy
210 viruses early on, leading to their divergence over more than 450 MY (23,38). Loss of activity in
211 other *SERINC*2 orthologs may have been associated with neofunctionalization: as suggested
212 by localized sequence divergence **(Fig-S14)**, presence of HNF4alpha binding enhancer **(Fig-**
213 **S15)** and change in tissue-specific expression patterns **(Fig-S16)** exemplified by expression of
214 *SERINC*2 in the liver of primates. Interestingly, Coelacanth *SERINC*2 inhibited HIV-1 and
215 remained invisible to the most powerful retroviral virulent factors nef (MAC239) and to the
216 glycoGag. Further studies can provide more insights into the lack of activity in these retroviral
217 factors and can be helpful in designing the modulators of the Nef-*SERINC* axis or designing
218 Nef-invisible *SERINC*s.
219 The ability of foamy virus envelope to counteract the restriction is first such evidence where a
220 canonical gene product is employed to evade *SERINC* restriction by these atypical retroviruses.
221 Foamy viruses co-diverged with their hosts and this consistently is also visible in their ability to
222 introduce variations in envelope glycoproteins among other documented genomic alterations.
223 Such changes perhaps are required for its efficient association with cognate entry receptors or
224 prevent host mechanisms from inhibiting the virus propagation. The nature of many such
225 interactions remains to be clarified due to the unavailability of reagents to study the phenotype
226 in its native context. The counteraction phenotype associated with foamy envelope
227 demonstrated here is not unexpected due to following the reason. It has been earlier suggested
228 that *SERINC*5-mediated particle inhibition varies with the HIV-1 envelope from various isolates
229 (16,39,40); indicating envelope as a determinant for *SERINC*5-sensitivity to particle restriction
230 as also recently demonstrated in (ref 38). Moreover, in the case of EIAV and MLV envelope the
231 ability to resist *SERINC*5 action has been observed (16,18). A constant engagement of
232 *SERINC*5 by the host seem to have therefore acted as a driving force during the evolution of
233 these retroviruses. Having found foamy envelope-dependent activity among coelacanth
234 *SERINC*2 is therefore not surprising and is in agreement with previous reports (41,42)
235 suggesting an ability of envelope to interact with SERINC. As a result, an early challenge by
236 this host factor leading to subsequent divergence of foamy envelope towards insensitivity to
237 *SERINC* restriction. The change in foamy envelope glycoproteins among coelacanth
238 endogenous foamy virus and a prototype foamy attest these facts that there may have been a
239 selective pressure imposed by *SERINC*2. Different SERINC paralogs might have specialized
240 to restrain specific viruses leading to coevolution of viruses in response to specific paralog.

241 We foresee that weaker signatures, exemplified by *SERINC*s **(Fig-1D, S3)** despite the constant
242 challenge from viruses, could be due to the native functions endowed to such transmembrane
243 proteins where the adaptation through diversification in-response to the pathogen would result
244 in a loss of a core function (43). The poor signatures could also be because the antiretroviral
245 activity is spread out over multiple host genes e.g. as a recent report shows that a Nef-sensitive
246 TIM1 activity is potentiated by *SERINC*5 (44). The host, therefore, can afford such redundancy
247 without having to diversify much. Another example is TLRs where the extracellular domain
248 shows signatures of recurrent positive selection in contrast to the conserved membrane-
249 spanning region (9). Intriguingly, virus specific TLRs are under stronger purifying selection than
250 non-viral TLRs (45) potentially due to the larger number of PAMPs associated with non-viral
251 pathogens. This constraint however may be more pronounced in SERINCs as they are multi-
252 pass transmembrane proteins known to inhibit only retroviruses. This nevertheless is indicative
253 of more *SERINC*-like restriction factors that display poor signatures of arms-race but are
254 functionally active. The core function of *SERINC*s in eukaryotes awaits independent
255 observations nevertheless, the most recent effort in providing structural insights into the fly and
256 human ortholog (41) opens up avenues for structure-inspired biological perturbations.
257 Despite being conserved, SERINCs have managed to diversify their function against distinct
258 retroviruses. In order to explain these dynamics of *SERINC*-retrovirus evolution, we first
259 collated all the known interactions of SERINCs with retroviral factors (**Fig-5A**). Since SERINC1
260 and SERINC4 are not translated from the native transcripts in the conditions that have been
261 probed, we reasoned that their presence might have been associated with extinct retroviral
262 factors. Investigation of SERINC1 and SERINC4 orthologs in diverse species, might be able to
263 decipher the proposed interactions (**Fig-5A**). In contrast to SERINC1 and SERINC4, we find
264 evidence for SERINC2 being counteracted by retroviral factor from foamy virus. Having
265 investigated all the available data, we decided to propose a model of co-evolution between
266 SERINCs and retroviruses that could explain the diversification of function despite weak
267 signatures of arms-race. Host-driven changes to the viral genome sequence is similar to niche-
268 filling models used to explain evolution of phenotypic traits (46). Hence, we reasoned that
269 divergence of SERINC paralogs following WGD would result in divergence of the niches a virus
270 can occupy. Not surprisingly, we find that viruses have evolved two types of retroviral
271 antagonists to resist SERINC restriction. These types reflect the distinct niches that viruses can
272 occupy. In contrast to previously proposed host-driven models of virus evolution characterized
273 by host adaptation and host-switches, our model suggests creation of host-niches within the
274 same organism due to divergence of paralogous gene copies. We illustrate our model using
275 the example of post-WGD diversification of interaction between SERINCs and distinct types of
276 retroviral factors (**Fig-5B**).
277
278 In conclusion, evolution-guided analysis for tracking the origin of anti-viral activity in the
279 *SERINC* genes and the dynamics following whole-genome duplication have identified the
280 presence of antiretroviral activity in the only *SERINC* thought to be deficient. The ancient

281 antiretroviral activity among *SERINC*s seems to have challenged retroviruses for more than
282 450 MY, as suggested by the presence of an evasion strategy in a spumavirus representative
283 to target coelacanth *SERINC*2. Finally, more insights into the mechanism of *SERINC*-mediated
284 restriction may enable therapeutic targeting of this evolutionarily conserved host-virus axis.
285

286 **Materials and Methods**

287 **Plasmids and reagents**

288 All the plasmids used were isolated using MN NucleoBond® Xtra Midi EF according to the
289 manufacturer's instructions to minimize endotoxin content. The list of plasmids and reagents
290 used in the experiments are tabulated in ***Supplementary Table I and II***.
291

292 **Cell lines**

293 All cell lines used were assessed for mycoplasma contamination and were found to be negative.
294 HEK293T and TZM-GFP indicator cell lines (previously described in Ref (16) were grown in
295 Dulbecco's Modified Eagle's Medium (DMEM) with 10% heat-inactivated Fetal Bovine Serum),
296 2mM L-Glutamine and 1% Penicillin-Streptomycin. Jurkat-TAg$^{SERINC3/5KO}$were reported
297 previously (18), maintained in RPMI 1640 with 10% FBS and 2mM L-Glutamine. All the cultures
298 were maintained at 37^{0}C and 5% CO2 in a humidified incubator.
299

300 **Viruses and infectivity assay**

301 HIV-1 was produced from HEK293T by calcium phosphate transfection and were limited to
302 single-cycle replication. For a 10 cm plate, 7ug NL4-3 env defective and nef defective, 1ug env
303 expressing plasmid and 100ng of pcDNA vectors expressing *SERINC* paralogs and orthologs
304 or equivalent empty vector and 1ug of PBJ6 *SERINC*5 HA was used for virus production. For
305 production of foamy viruses, transient transfection of 0.736 ug pCIES, 1.5ug pCIPS, 11.84ug
306 pCIGS, 11.84 ug pΔΦ and 100ng of pcDNA vectors expressing *SERINC* paralogs and
307 orthologs or equivalent control vector in HEK293T(10 cm plate) was done (47). The viral
308 particles were collected 48 hours post transfection and were centrifuged at 300g for 5 min and
309 quantified by SG-PERT reverse transcription assay (48). Following this, viruses were serially
310 diluted 3, 9 and 27-fold for infection in TZM-GFP reporter cells that were seeded in a 96-well
311 plate, 24 hours prior to infection. HIV-1 Infectivity was quantified by scoring the GFP positive
312 cells using Spectra max MiniMax^{TM} 300 imaging Cytometer (Molecular devices, USA). Foamy
313 Virus infectivity was examined by the number of GFP positive cells indicating the population
314 transduced by Foamy virus. The total cell population was analyzed by nuclei staining with
315 Hoechst 33342 and visualized on CellInsight CX7 High Content Screening platform (Thermo
316 Scientific). The acquired values were normalized with the virus titre obtained from SG-PERT
317 assay as previously described (16) Results are expressed as a percentage of an internal control
318 sample.
319

320 **Immunofluorescence**

321 For electroporation in JTag$^{SERINC3/5KO}$, cells were grown, and fresh medium was added a day
322 before such that the culture concentration did not exceed 10^6 cells/ml. Cells in their exponential
323 growth phase were pellet down (10^7 cells/sample) at 300xg for 10 mins. Prior to adding Opti-
324 MEM, the cells were washed with 1X Phoshphate Buffered Saline (PBS (1X) pH 7.0) to remove
325 residual serum and other cell debris. Each sample was resuspended in 200ul warm
326 OptiMEM. 5ug of constructs expressing HA-tagged *SERINC*2 orthologs or equivalent control
327 vector were then added to the cells. The cells and DNA mixture are added to a 0.2cm gap
328 electroporation cuvette. The cells were pulsed at 140V and 1000uF with exponential decay on
329 BioRAD GenePulser Xcell. 600ul warm RPMI with 20% FBS was immediately added to the
330 electroporated cells, following which they were transferred to a plate containing RPMI with 10%
331 FBS. 48 hours post transfection cells were pellet down at 300g for 5 mins and resuspended
332 in100ul RPMI and laid on poly-L-lysine coated coverslips and fixed with 4% paraformaldehyde.
333 After fixation, the cells were washed twice with 1X PBS. The cells were permeabilized using
334 BD™Perm/wash followed by detection of HA tag with Purified anti-HA.11 Epitope Tag Antibody
335 and Alexa 488 fluorescent tagged secondary antibody. The coverslips were transferred to a
336 glass slide and mounted using ProLong™ Glass Antifade reagent. Images were acquired after
337 12 hours on Zeiss confocal microscope (LSM740).
338
339 **Virus incorporation**
340 Viruses were produced by calcium phosphate transfection in a 10cm plate of HEK293T as
341 mentioned above. The media was replaced with DMEM containing 2% FBS after 12-15 hours
342 of transfection. After 48 hours, the virus containing supernatant was collected and centrifuged
343 at 500xg for 10 mins to exclude any cell fragments. Following this, the viruses were filtered
344 using a 0.22µm syringe filter. This was overlaid on 25% sucrose cushion and concentrated at
345 50000xg for 2 hours at 4 degrees using a Beckmann Coulter ultracentrifuge. After the spin, the
346 supernatant was aspirated off and the pellet was lysed in Laemmli buffer with TCEP.
347
348
349 **Western blotting**
350 After collection of viruses from producer cells (HEK293T), the cells were collected in 1X ice-
351 cold PBS. They were washed twice at 500g for 5 minutes. The PBS was aspirated until the
352 pellet was completely dry. The pellets were either processed for lysis or stored in -80 until
353 further application. The cell pellets were lysed in DDM Lysis buffer (100mM NaCl, 10mM
354 HEPES pH 7.5, 50mM Tris(2-carboxyethyl) phosphine hydrochloride (TCEP), 1% n-Dodecyl-
355 β-D-maltoside (DDM), 2xcOmplete™, EDTA-free Protease inhibitor cocktail and rocked on ice
356 for 30 minutes. Following this, the lysates were centrifuged at 10000g for 15 mins and the
357 supernatant was collected and mixed with 4x Laemmli buffer with 10mM TCEP.
358 SDS-PAGE was used for resolving cell pellets and virions for analysis by western blot. The
359 proteins from the gel were transferred onto a PVDF membrane on a semi-dry transfer unit
360 (Hoefer TE77) for 75 minutes with 125 Amp constant current. The membrane containing the

361 proteins was then blocked with 2x Odyssey Blocking Buffer that was diluted with 1x TBS to
362 make 1x Blocking buffer. After 20 minutes of blocking, Anti-HA.11 Epitope Tag Antibody
363 (mouse) and anti-actin(rabbit) (diluted 1: 1000 in 1x blocking buffer) was used to probe the
364 membrane to detect the *SERINC* orthologs and paralogs that were tagged with C-terminal HA
365 tag. After incubation with the primary antibody for 1 hour, the membrane was washed thrice
366 with 1X TBST for 5 mins. Goat anti-mouse 680 and goat anti-rabbit 800 Li-Cor antibodies were
367 used to detect infra-red dyes signal from the membrane. The western blot was analysed on
368 Odyssey imager system.
369
370 **Reconstruction of coelacanth *SERINC*5 sequence**
371 The *SERINC*5 from coelacanth was found to be shorter than its annotation from its orthologs.
372 Upon closer inspection it was found that the exons orthologous to human exons1-3 were
373 missing in the coelacanth *SERINC*5 genomic sequence. We found that the upstream region of
374 coelacanth *SERINC*5 had a gap in the genomic sequence. It was also found that the transcribed
375 regions upstream of the gap did not correspond to *SERINC*5 exons. Hence, we decided to use
376 a chromosome walking strategy to reconstruct the missing exons, such that at least at
377 sequence level the topology of the protein could be studied (suppl material for reconstruction
378 of *SERINC*5).
379
380 **Data and code availability**
381 The multiple sequence alignments are available for download under GNU license from the
382 github repository https://github.com/ceglab/RestrictionFactorsArmsRace.
383
384 **Genome correction and quality check**
385
386 In order to rule out the possibility of artefacts in evolutionary analysis that arise from errors in
387 the sequence of genome assemblies (true even for high quality reference genomes found on
388 ensemble(49)) we systematically assessed the quality of each of the primate genomes used in
389 this study. Genome assemblies of 15 primate species were downloaded from ensembl release
390 98 through the ftp site. Whole genome sequencing datasets corresponding to each of these
391 species were obtained from the Short Read Archive (SRA) with the criteria that they should
392 have >~30x coverage. Details of the genome assemblies used and the corresponding raw read
393 data from each species are provided in GitHub repository. The raw read data were mapped to
394 the corresponding genomes using the bwa mem read mapper(50) with default settings. The
395 alignment files obtained from the mapping step were used to generate the genotype likelihood
396 estimates using the program angsd (51). The genotype likelihood estimates were provided to
397 the program referee(52) to assign quality scores and perform genome correction. Overall, we
398 found that in all the primate genomes considered, less than 1% of the bases were corrected by
399 the program referee. The sequencing data used for performing genome correction are not from

the same individual that was used for genome assembly. Hence, it is possible that many of the corrected positions are merely nucleotide polymorphisms.

Manual curation and multiple sequence alignment

The manually curated open reading frame multi-fasta files consisting of 70 genes from ~15 primate species were collected from Ensembl. We extend our previous multiple sequence alignment strategy(53) by including additional multiple sequence alignment programs to generate 8 independent alignments for each gene. Several multiple sequence alignment tools were used to ensure that the inferred patterns of sequence evolution are not restricted to the alignment strategy used. The choice of the actual multiple sequence alignment tools used was based on the performance-based classification of algorithms (54).

Use of FUBAR to find evolutionary fingerprints

Traditional approaches that endeavour to find arms race signatures in genes look for recurrent occurrence of positive selection in the same gene in different evolutionary lineages. A more recent approach has been to use the full joint distribution of synonymous (α) and nonsynonymous (β) rates as an evolutionary fingerprint of a gene(19). The program FUBAR(55) is available as part of the HyPhy package(56). Pairs of conditionally dependent sites were identified using the program BGM(57). Estimates of selection coefficients are inferred from the multiple sequence alignments for pairs of α- β combinations that form a discretized grid. We calculated the distance measure defined by Murrel(19) to perform hierarchical clustering of the selection signatures obtained from FUBAR.

Acknowledgements

This work is supported by IYBA fellowship (BT/010/IYBA/2017/01), a grant (BT/PR26013/GET/119/191/2017) from the Department of Biotechnology, Government of India, and the Wellcome Trust/DBT India Alliance Fellowship [grant number IA/I/18/2/504006 awarded to AC]. PR, VB and AS are supported by a fellowship from the MHRD, CSIR and DBT respectively. The computational analyses were performed on the Har Gobind Khorana Computational Biology cluster. Authors thank Jeremy Luban, and the NIH AIDS Reagent Program for the reagents and cell lines. Authors are grateful to Massimo Pizzato for his critical inputs and reagent support.

References

1. Koonin E V., Dolja V V., Krupovic M. Origins and evolution of viruses of eukaryotes: The ultimate modularity. Virology. 2015.

2. Malfavon-Borja R, Sawyer SL, Wu LI, Emerman M, Malik HS. An evolutionary screen highlights canonical and noncanonical candidate antiviral genes within the primate TRIM gene family. Genome Biol Evol. 2013;

440 3. Paparisto E, Woods MW, Coleman MD, Moghadasi SA, Kochar DS, Tom SK, et al.
441 Evolution-Guided Structural and Functional Analyses of the HERC Family Reveal an
442 Ancient Marine Origin and Determinants of Antiviral Activity. J Virol. 2018;

443 4. Daugherty MD, Schaller AM, Geballe AP, Malik HS. Evolution-guided functional
444 analyses reveal diverse antiviral specificities encoded by ifit1 genes in mammals. Elife.
445 2016;

446 5. Sackton TB, Lazzaro BP, Clark AG, Wittkopp P. Rapid expansion of immune-related
447 gene families in the house fly, musca domestica. Mol Biol Evol. 2017;

448 6. Kasahara M. Genome Duplication and T Cell Immunity. In: Progress in molecular
449 biology and translational science. 2010. p. 7–36.

450 7. Dehal P, Boore JL. Two Rounds of Whole Genome Duplication in the Ancestral
451 Vertebrate. Holland P, editor. PLoS Biol. 2005 Sep;3(10):e314.

452 8. Duggal NK, Emerman M. Evolutionary conflicts between viruses and restriction factors
453 shape immunity. Nat Rev Immunol. 2012;12(10):687–95.

454 9. Wlasiuk G, Khan S, Switzer WM, Nachman MW. A history of recurrent positive
455 selection at the toll-like receptor 5 in primates. Mol Biol Evol. 2009;

456 10. Daugherty MD, Young JM, Kerns JA, Malik HS. Rapid Evolution of PARP Genes
457 Suggests a Broad Role for ADP-Ribosylation in Host-Virus Conflicts. PLoS Genet.
458 2014;

459 11. Boso G, Buckler-White A, Kozak CA. Ancient Evolutionary Origin and Positive
460 Selection of the Retroviral Restriction Factor Fv1 in Muroid Rodents . J Virol. 2018;

461 12. Compton AA, Malik HS, Emerman M. Host gene evolution traces the evolutionary
462 history of ancient primate lentiviruses. Philosophical Transactions of the Royal Society
463 B: Biological Sciences. 2013.

464 13. Harris RS, Hultquist JF, Evans DT. The restriction factors of human immunodeficiency
465 virus. Journal of Biological Chemistry. 2012.

466 14. McLaren PJ, Gawanbacht A, Pyndiah N, Krapp C, Hotter D, Kluge SF, et al.
467 Identification of potential HIV restriction factors by combining evolutionary genomic
468 signatures with functional analyses. Retrovirology. 2015;

469 15. Firrito C, Bertelli C, Vanzo T, Chande A, Pizzato M. SERINC5 as a New Restriction
470 Factor for Human Immunodeficiency Virus and Murine Leukemia Virus. Annu Rev
471 Virol. 2018;

472 16. Rosa A, Chande A, Ziglio S, De Sanctis V, Bertorelli R, Goh SL, et al. HIV-1 Nef
473 promotes infection by excluding SERINC5 from virion incorporation. Nature.
474 2015;526(7572):212–7.

475 17. Usami Y, Wu Y, Göttlinger HG. SERINC3 and SERINC5 restrict HIV-1 infectivity and
476 are counteracted by Nef. Nature. 2015;526(7572):218–23.

477 18. Chande A, Cuccurullo EC, Rosa A, Ziglio S, Carpenter S, Pizzato M. S2 from equine
478 infectious anemia virus is an infectivity factor which counteracts the retroviral inhibitors
479 SERINC5 and SERINC3. Proc Natl Acad Sci U S A. 2016;113(46).

480 19. Murrell B, Vollbrecht T, Guatelli J, Wertheim JO. The Evolutionary Histories of
481 Antiretroviral Proteins SERINC3 and SERINC5 Do Not Support an Evolutionary Arms
482 Race in Primates. J Virol. 2016 Jun 29;

483 20. Shaw AE, Hughes J, Gu Q, Behdenna A, Singer JB, Dennis T, et al. Fundamental
484 properties of the mammalian innate immune system revealed by multispecies

485 comparison of type I interferon responses. PLoS Biol. 2017;

486 21. Lynch M. The Age and Relationships of the Major Animal Phyla. Evolution (N Y).
487 1999;

488 22. Ahmad I, Li S, Li R, Chai Q, Zhang L, Wang B, et al. The retroviral accessory proteins
489 S2, Nef, and glycoMA use similar mechanisms for antagonizing the host restriction
490 factor SERINC5. J Biol Chem. 2019;

491 23. Han GZ, Worobey M. An endogenous foamy-like viral element in the coelacanth
492 genome. PLoS Pathog. 2012;

493 24. Sawyer SL, Wu LI, Emerman M, Malik HS. Positive selection of primate
494 TRIM5 identifies a critical species-specific retroviral restriction domain. Proc Natl
495 Acad Sci. 2005;

496 25. Newman RM, Hall L, Connole M, Chen G-L, Sato S, Yuste E, et al. Balancing
497 selection and the evolution of functional polymorphism in Old World monkey TRIM5 .
498 Proc Natl Acad Sci. 2006;

499 26. McLaughlin RN, Gable JT, Wittkopp CJ, Emerman M, Malik HS. Conservation and
500 Innovation of APOBEC3A Restriction Functions during Primate Evolution. Mol Biol
501 Evol. 2016;

502 27. Johnson WE. Rapid adversarial co-evolution of viruses and cellular restriction factors.
503 Curr Top Microbiol Immunol. 2013;

504 28. Blanco-Melo D, Venkatesh S, Bieniasz PD. Origins and Evolution of tetherin, an
505 Orphan Antiviral Gene. Cell Host Microbe. 2016 Aug 10;20(2):189–201.

506 29. Meng X, Zhang F, Yan B, Si C, Honda H, Nagamachi A, et al. A paralogous pair of
507 mammalian host restriction factors form a critical host barrier against poxvirus
508 infection. PLoS Pathog. 2018;

509 30. Browne EP, Littman DR. Species-Specific Restriction of Apobec3-Mediated
510 Hypermutation. J Virol. 2008;

511 31. Mitchell PS, Patzina C, Emerman M, Haller O, Malik HS, Kochs G. Evolution-guided
512 identification of antiviral specificity determinants in the broadly acting interferon-
513 induced innate immunity factor MxA. Cell Host Microbe. 2012;

514 32. Mitchell PS, Young JM, Emerman M, Malik HS. Evolutionary Analyses Suggest a
515 Function of MxB Immunity Proteins Beyond Lentivirus Restriction. PLoS Pathog. 2015;

516 33. Irwin B, Aye M, Baldi P, Beliakova-Bethell N, Cheng H, Dou Y, et al. Retroviruses and
517 yeast retrotransposons use overlapping sets of host genes. Genome Res. 2005;

518 34. Miller JE, Zhang L, Jiang H, Li Y, Pugh BF, Reese JC. Genome-wide mapping of
519 decay factor-mRNA interactions in yeast identifies nutrient-responsive transcripts as
520 targets of the deadenylase Ccr4. G3 Genes, Genomes, Genet. 2018;

521 35. Llorens J V., Clark JB, Martínez-Garay I, Soriano S, De Frutos R, Martínez-Sebastián
522 MJ. Gypsy endogenous retrovirus maintains potential infectivity in several species of
523 Drosophilids. BMC Evol Biol. 2008;

524 36. Teysset L, Burns JC, Shike H, Sullivan BL, Bucheton A, Terzian C. A Moloney Murine
525 Leukemia Virus-Based Retroviral Vector Pseudotyped by the Insect Retroviral gypsy
526 Envelope Can Infect Drosophila Cells. J Virol. 1998;

527 37. Mellor J, Fulton SM, Dobson MJ, Wilson W, Kingsman SM, Kingsman AJ. A retrovirus-
528 like strategy for expression of a fusion protein encoded by yeast transposon Ty1.
529 Nature. 1985;

530 38. Aiewsakun P, Katzourakis A. Marine origin of retroviruses in the early Palaeozoic Era.
531 Nat Commun. 2017;

532 39. Beitari S, Ding S, Pan Q, Finzi A, Liang C. The effect of HIV-1 Env on SERINC5
533 antagonism. J Virol [Internet]. 2016;(December):JVI.02214-16. Available from:
534 http://jvi.asm.org/lookup/doi/10.1128/JVI.02214-16

535 40. Sood C, Marin M, Chande A, Pizzato M, Melikyan GB. SERINC5 protein inhibits HIV-1
536 fusion pore formation by promoting functional inactivation of envelope glycoproteins. J
537 Biol Chem [Internet]. 2017 Apr 7 [cited 2017 May 26];292(14):6014–26. Available
538 from: http://www.ncbi.nlm.nih.gov/pubmed/28179429

539 41. Pye, V.E., Rosa, A., Bertelli C et al. A bipartite structural organization defines the
540 SERINC family of HIV-1 restriction factors. Nat Struct Mol Biol. 2020;27:78–83.

541 42. Beitari S, Ding S, Pan Q, Finzi A, Liang C. Effect of HIV-1 Env on SERINC5
542 Antagonism. J Virol. 2017;91(4).

543 43. Sojo V, Dessimoz C, Pomiankowski A, Lane N. Membrane Proteins Are Dramatically
544 Less Conserved than Water-Soluble Proteins across the Tree of Life. Mol Biol Evol.
545 2016;

546 44. Li M, Waheed AA, Yu J, Zeng C, Chen HY, Zheng YM, et al. TIM-mediated inhibition
547 of HIV-1 release is antagonized by Nef but potentiated by SERINC proteins. Proc Natl
548 Acad Sci U S A. 2019;

549 45. Liu G, Zhang H, Zhao C, Zhang H. Evolutionary History of the Toll-Like Receptor
550 Gene Family across Vertebrates. Enard D, editor. Genome Biol Evol [Internet]. 2020
551 Jan 1 [cited 2020 Feb 7];12(1):3615–34. Available from:
552 https://academic.oup.com/gbe/article/12/1/3615/5652095

553 46. Simmonds P, Aiewsakun P, Katzourakis A. Prisoners of war — host adaptation and its
554 constraints on virus evolution. Nat Rev Microbiol. 2019;

555 47. Trobridge G, Josephson N, Vassilopoulos G, Mac J, Russell DW. Improved foamy
556 virus vectors with minimal viral sequences. Mol Ther. 2002;6(3):321–8.

557 48. Pizzato M, Erlwein O, Bonsall D, Kaye S, Muir D, McClure MO. A one-step SYBR
558 Green I-based product-enhanced reverse transcriptase assay for the quantitation of
559 retroviruses in cell culture supernatants. J Virol Methods [Internet]. 2009 Mar [cited
560 2017 Jun 19];156(1–2):1–7. Available from:
561 http://www.ncbi.nlm.nih.gov/pubmed/19022294

562 49. Mittal P, Jaiswal SK, Vijay N, Saxena R, Sharma VK. Comparative analysis of
563 corrected tiger genome provides clues to its neuronal evolution. Sci Rep [Internet].
564 2019 Dec 5 [cited 2020 Jan 13];9(1):18459. Available from:
565 http://www.nature.com/articles/s41598-019-54838-z

566 50. Li H. [Heng Li - Compares BWA to other long read aligners like CUSHAW2] Aligning
567 sequence reads, clone sequences and assembly contigs with BWA-MEM. arXiv Prepr
568 arXiv. 2013;

569 51. Korneliussen TS, Albrechtsen A, Nielsen R. ANGSD: Analysis of Next Generation
570 Sequencing Data. BMC Bioinformatics. 2014;

571 52. Thomas GWC, Hahn MW. Referee: Reference assembly quality scores. Genome Biol
572 Evol. 2019;

573 53. Shinde SS, Teekas L, Sharma S, Vijay N. Signatures of Relaxed Selection in the
574 CYP8B1 Gene of Birds and Mammals. J Mol Evol. 2019;

575 54. Blackburne BP, Whelan S. Class of multiple sequence alignment algorithm affects

576 genomic analysis. Mol Biol Evol. 2013;

577 55. Murrell B, Moola S, Mabona A, Weighill T, Sheward D, Kosakovsky Pond SL, et al.
578 FUBAR: A fast, unconstrained bayesian AppRoximation for inferring selection. Mol
579 Biol Evol. 2013;

580 56. Kosakovsky Pond SL, Frost SDW, Muse S V. HyPhy: Hypothesis testing using
581 phylogenies. Bioinformatics. 2005;

582 57. Avino M, Poon AFY. Detecting Amino Acid Coevolution with Bayesian Graphical
583 Models. In: Methods in Molecular Biology. 2019.

584

585 **Figure Legends**

586

587 **Figure 1**. The activity of *SERINC* paralogs and orthologs on HIV-1 infectivity

588 A) The activity of Human *SERINC* paralogs (*SERINC*1-*SERINC*5) on nef-defective HIV-
589 1 Infectivity. (n=4, mean ± s.d., unpaired t-test, (*)p<0.05 (**)p<0.01 (***)p<0.001, ns-
590 not significant). Lower panel, Western blot showing expression of c-terminally HA-
591 tagged *SERINC* and the corresponding B-actin from cell lysate (HEK293T). Values
592 obtained from the empty vector control was normalized to 100% for comparison with
593 *SERINC* expressors
594 B) Representative images of TZM-GFP cells infected with viruses produced for Fig-1A.
595 Cells are stained with Hoechst and captured at 10x magnification on Cell Insight CX7
596 High Content Screening platform
597 C) Immunofluorescence assay for the indicated HA-tagged human *SERINC*1-5
598 transfected in JTAg *SERINC*5/3$^{-/-}$ cells and visualized using Alexa 488 secondary
599 antibody
600 D) Hierarchical clustering of the arms-race signatures in primate genes aligned using
601 ClustalW aligner and used as input for FUBAR. Interferon-induced genes identified by
602 (Shaw et al 2017) are color-coded as red (upregulated), blue(downregulated), green
603 (*SERINC* paralogs), grey (other select genes)
604 E) The activity of pre-and-post-WGD *SERINC5* orthologs on nef-defective HIV-1
605 infectivity. (n=4, mean ± s.d., unpaired t-test, (*)p<0.05 (**)p<0.01 (***)p<0.001, ns-
606 not significant). Lower panel, Western blot showing expression of indicated orthologs
607 tagged with HA and the corresponding B-actin from cell lysate (HEK293T)
608 F) Representative images of TZM-GFP cells infected with viruses produced for Fig-1E.
609 Cells are stained with Hoechst and captured at 10x magnification on Cell Insight CX7
610 High Content Screening platform
611 G) Immunofluorescence assay for indicated HA-tagged *SERINC* orthologs transfected in
612 JTAg *SERINC*5/3$^{-/-}$ cells and visualized using Alexa 488 secondary antibody.

613 **Figure 2**- Coelacanth *SERINC*2 inhibits HIV-1 infectivity

614 A. A Schematic timeline depicting the sequence of events during the course of evolution
615 with species depicted from left to right being *S. cerevisiae, D. melanogaster, L.*
616 *chalumnae, X. tropicalis, G.gallus, E. caballus, M. musculus* and *H. sapiens*
617 B. The activity of *SERINC*2 from coelacanth and human *SERINC*2 isoforms on nef-
618 defective HIV-1 infectivity. Values obtained from the empty vector control was
619 normalized to 100% for comparison with *SERINC* expressors. (n=4, mean ± s.d.,
620 unpaired t-test, (*) p<0.05 (**)p<0.01 (***)p<0.001, ns-not significant). Lower panel,
621 Representative images of TZM-GFP cells infected with viruses produced for top
622 panel. Cells are stained with Hoechst and captured at 10x magnification on
623 CellInsight CX7 High Content Screening platform.
624 C. The activity of *SERINC*2 orthologs from coelacanth, xenopus, gallus, mus, equus and
625 human on nef-defective HIV-1 infectivity. Values obtained from the empty vector
626 control was normalized to 100% for comparison with *SERINC* expressors. (n=4,

627 mean ± s.d., unpaired t-test, (*)p<0.05 (**)p<0.01 (***)p<0.001, ns-not significant).
628 Lower panel, western blot showing expression of *SERINC*2 orthologs tagged with HA
629 and the corresponding B-actin from cell lysate (HEK293T).
630 D. Representative images of TZM-GFP cells infected with viruses produced for Fig-2C.
631 Cells are stained with Hoechst and captured at 10x magnification on Cell Insight CX7
632 High Content Screening platform
633 E. Immunofluorescence from for indicated HA-tagged *SERINC* orthologs transfected in
634 JTAg *SERINC*5/3$^{-/-}$ cells and visualized using Alexa 488 secondary antibody

635 **Figure 3-** The ability of retroviral factors to antagonize *SERINC*s

636 A. The ability of Nef and glycoGag to counteract indicated *SERINC*2 orthologs. Human
637 *SERINC*5 was served as control for Nef and glycoGag counteraction of the
638 restriction. Values obtained from the empty vector control without Nef or glycoGag
639 was normalized to 100% for comparison with *SERINC* expressors
640 B. Representative images of TZM-GFP cells infected for viruses produced for Fig-3A.
641 Cells are stained with Hoechst and captured at 10x magnification on Cell Insight CX7
642 High Content Screening platform
643 C. The ability of nef alleles to antagonize indicated *SERINC*2 orthologs. Human
644 *SERINC*5 is used as a control
645 D. Susceptibility of HIV-1 clade-B (HXB2 and JR-FL), clade-C (ZM109F, CAP210) and
646 VSV envelope glycoprotein (VSV-G) to inhibition of infectivity by coelacanth
647 *SERINC*2 with human *SERINC*2 and *SERINC*5 as controls.
648 E. Phylogenetic tree depicting the relationship among various retroviruses. Unknown
649 retroviral interactions with *SERINC*s are shown in the black ellipse while the known
650 ones are in blue. Branches colored red are complex lentiviruses, blue are gamma
651 retroviruses and green are foamy viruses.

652 **Figure 4**- The effect of Coelacanth *SERINC*2 on Foamy virus infectivity and antagonism by
653 the envelop glycoprotein

654 A. Genome organization of an endogenous foamy virus (CoeFV) from coelacanth and
655 the prototype foamy virus (FV)

656 B. Infectivity of foamy virus-derived vector and a nef-defective HIV-1 in the presence of
657 indicated human *SERINC* paralogs and *SERINC*2 orthologs. Foamy virus and HIV-1
658 infectivity obtained from the empty vector control was normalized to 100% for
659 comparison with *SERINC* expressors

660 C. Nef-defective HIV-1 infectivity obtained from the empty vector control, normalized to
661 100% for comparison, and with human *SERINC*5. Each foamy virus plasmids
662 expressing different components (gag, pol and env) along with the transfer vector
663 (pδϕ) were used for its ability to counteract human *SERINC*5. SIV MAC239 Nef was
664 used as a control. Lower panel, representative images of TZM-GFP cells infected
665 with viruses produced for Fig-4C. Cells are stained with Hoechst and captured at 10x
666 magnification on CellInsight CX7 High Content Screening platform.
667

668 D. Nef-defective HIV-1 infectivity obtained from the empty vector control, normalized to
669 100% for comparison, and with Coelacanth *SERINC*2. Each foamy virus plasmids
670 expressing different components (gag, pol and env) along with the transfer vector
671 (pδϕ) were used for its ability to counteract Coelacanth *SERINC*2. Lower panel,
672 representative images of TZM-GFP cells infected with viruses produced for Fig-4D.
673 Cells are stained with Hoechst and captured at 10x magnification on CellInsight CX7
674 High Content Screening platform.

675 E. Western blot showing varying expression of Coelacanth *SERINC*2-HA (from PBJ6
676 and pcDNA vectors) and the corresponding B-actin from cell lysate (HEK293T) in the
677 presence and absence of Foamy virus envelope expressor.

678 F. The sensitivity of the foamy core to the action of coelacanth *SERINC*2. The foamy

core was trans-complemented with either Foamy envelope, HIV-1 envelope or HIV-1 envelope lacking a c-terminal domain and indicated SERINC was co-expressed to check the ability of individual SERINC to restrict foamy virus. (n = 4, mean ± s.d., unpaired t-test).

Figure-5. Schematic representation of *SERINC*-retrovirus interactions

A. *SERINC* antagonists (glycoGag, Nef and S2) from distant retroviruses. An interaction between known and hypothesized virulent factors with *SERINC* paralogs. Solid lines show experimentally demonstrated interactions while the dotted lines represent hypothesized interactions. Color-coding for extinct and extant virulent factors (VF). Extinct VFs are shown in light blue, the extant VFs (Type-1) are in purple and Type-2 are in black.

B. A proposed model for adaptive co-evolution among retroviral factors and SERINCs. The evolution of patterns of interactions between viral factors and SERINCs have diversified following post-whole-genome duplication.

Supplementary Figure Legends

Figure S1- Phylogenetic analysis of SERINC paralogs**.** *S. cerevisiae, C. elegans, and D. melanogaster* has a single copy of this gene. Whole-genome duplication that occurred in an early ancestor of mammals gave rise to a cluster of five genes divided into clusters of SERINC1, SERINC2, SERINC3, and SERINC4 and SERINC5. Colors denote different branches of each SERINC in chordates. The lengths of the triangles are proportional to the number of nucleotide substitutions that have taken place in a particular branch. The tree was generated using Ensembl.

Figure S2- Topology of human SERINC Paralogs predicted using TOPCONS

Figure S3- Arms-race signatures of primate SERINC genes inferred using FUBAR

Figure S4- Distribution of sites under different selection regimes across the SERINC genes. The colors are inner (Blue), outer (Pink), helix (Red). Black dots are estimates of dS and red dots are dN. Pairs of conditionally dependent sites identified by the program BGM (Bayesian Graphical Model) are connected by a dotted line (see SERINC1 and SERINC4). Vertical green lines correspond to the sites under purifying selection.

Figure S5- Effect of different aligners on hierarchical clustering of arms-race signatures of primate genes. Interferon induced genes identified by (Shaw et al 2017) are color coded as red (upregulated), blue(downregulated), green (SERINC paralogs), grey (other select genes)

Figure S6- Topology of SERINC5 orthologs predicted using Topcons. Coelacanth SERINC5 was reconstructed from the RNAseq data (*) see supplemental material for details

Figure S7- Topological features of Human SERINC2 splice isoforms and coelacanth SERINC2 predicted using TOPCONS

Figure S8- Topology of SERINC2 orthologs predicted using TOPCONS

Figure S9- Incorporation of SERINC2 orthologs in the virus particles and detection by indicted antibodies against target proteins

720 **Figure S10**- Effect of a dose-dependent expression of coelacanth SERINC2 on HIV-1
721 infectivity

722 **Figure S11**- Counteraction of coelacanth SERINC2 restriction by a Foamy virus envelope
723 glycoprotein

724 **Figure S12**- Reciprocal-packaging of a foamy envelope with an HIV core and sensitivity to
725 SERINCs

726 **Figure S13**- Infectivity of HIV-1 produced from JTAgSERINC5/3KO having ectopic
727 expression of the indicated SERINC

728 **Figure S14**- Multiple sequence alignment of SERINC2 orthologs; highlighted regions showing
729 the sites of sequence divergence

730 **Figure S15**- Evidence for the presence of HNF4a binding site in the intron of human
731 SERINC2 gene

732 **Figure S16**- Gene expression evolution of SERINC genes in vertebrates

733

734 **Supplementary Information:**

735 **Supplementary Table I:** List of plasmids used

736 **Supplementary Table II**: List of reagents used

737 Reconstruction of Coelacanth SERINC5

Figure 1

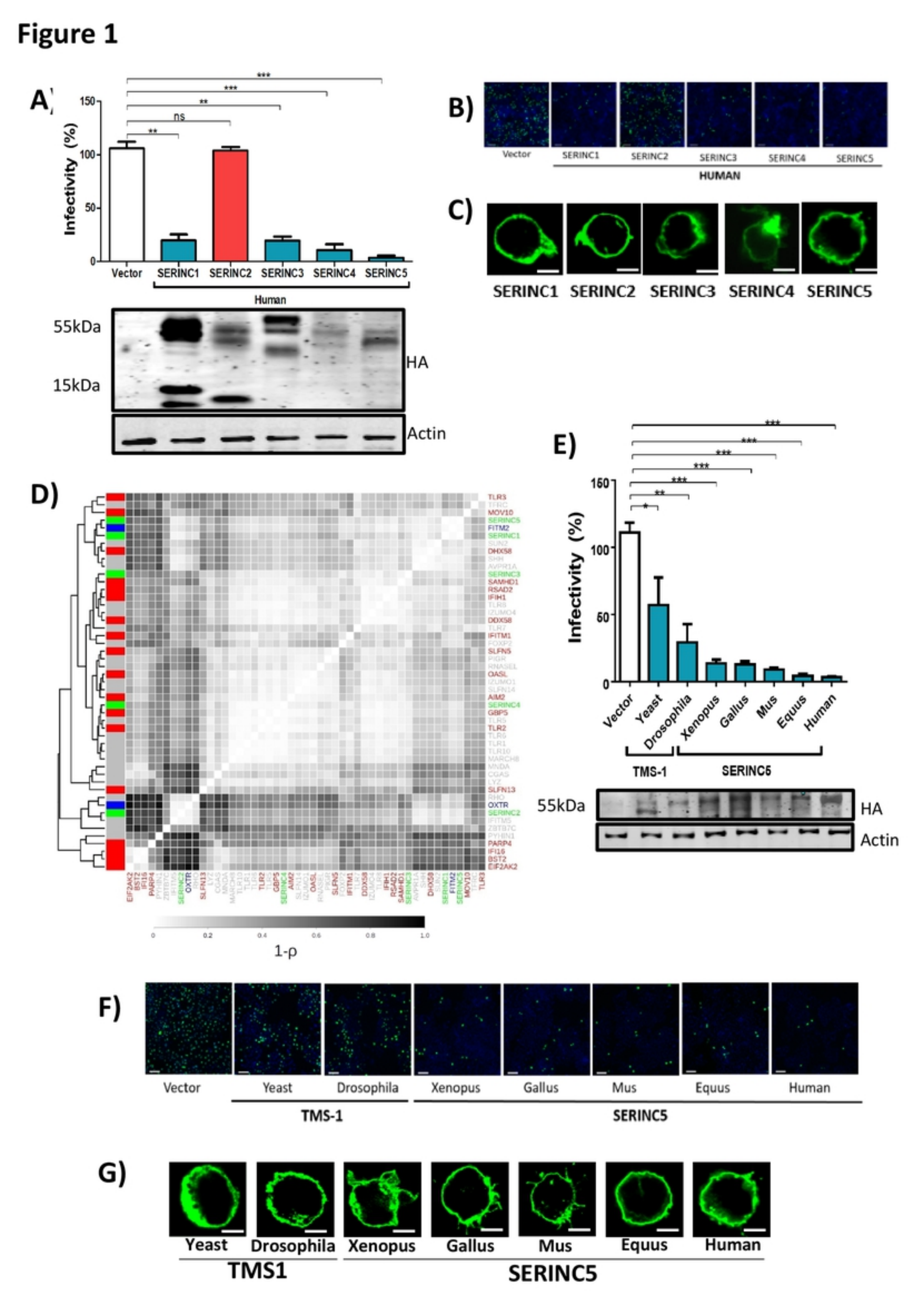
A)
Infectivity (%)
150
100
50
0
***
***
**
ns
**
Vector
SERINC1
SERINC2
SERINC3
SERINC4
SERINC5
Human
55kDa
15kDa
HA
Actin
B)
Vector
SERINC1
SERINC2
SERINC3
SERINC4
SERINC5
HUMAN
C)
SERINC1
SERINC2
SERINC3
SERINC4
SERINC5
D)
1-ρ
E)
Infectivity (%)
150
100
50
0
***
***
**
*
Vector
Yeast
Drosophila
Xenopus
Gallus
Mus
Equus
Human
TMS-1
SERINC5
55kDa
HA
Actin
F)
Vector
Yeast
Drosophila
Xenopus
Gallus
Mus
Equus
Human
TMS-1
SERINC5
G)
Yeast
Drosophila
Xenopus
Gallus
Mus
Equus
Human
TMS1
SERINC5

Figure 2

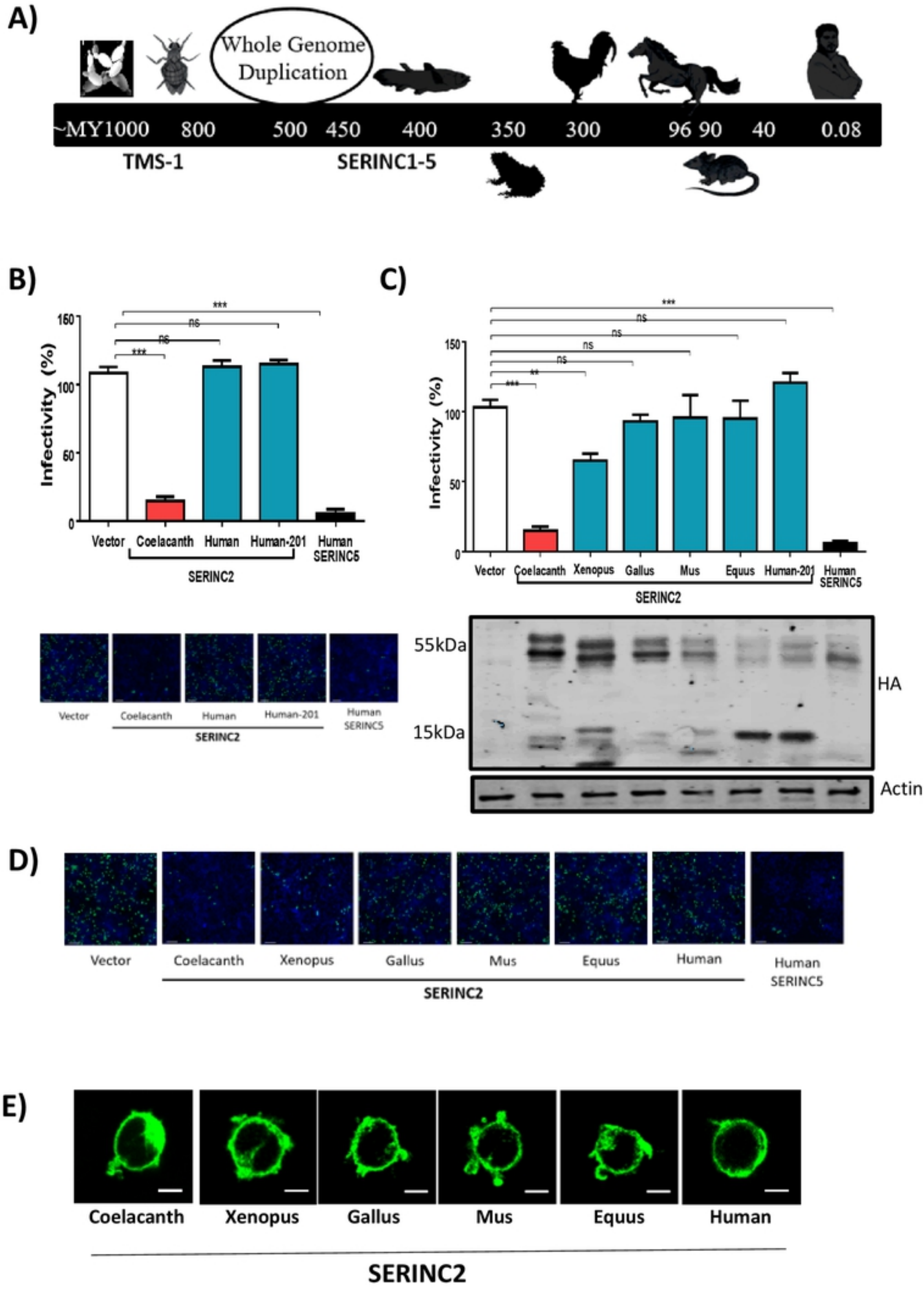
A)
Whole Genome Duplication
~MY1000
800
500
450
400
350
300
96
90
40
0.08
TMS-1
SERINC1-5
B)
Infectivity (%)
Vector
Coelacanth
Human
Human-201
Human SERINC5
SERINC2
C)
Infectivity (%)
Vector
Coelacanth
Xenopus
Gallus
Mus
Equus
Human-201
Human SERINC5
SERINC2
55kDa
15kDa
HA
Actin
D)
Vector
Coelacanth
Xenopus
Gallus
Mus
Equus
Human
Human SERINC5
SERINC2
E)
Coelacanth
Xenopus
Gallus
Mus
Equus
Human
SERINC2

Figure 3

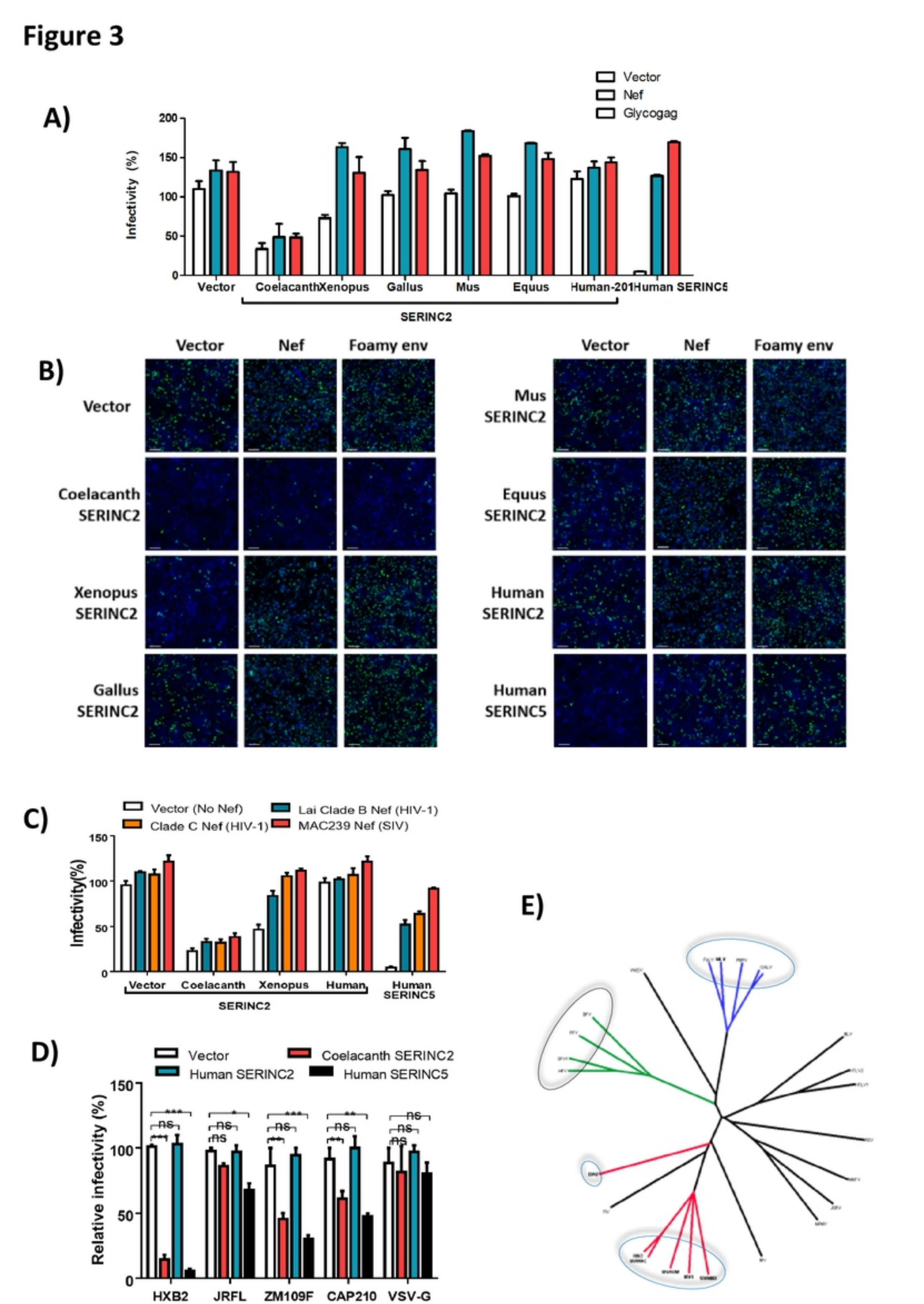
A)
Vector
Nef
Glycogag
Infectivity (%)
200
150
100
50
0
Vector
Coelacanth
Xenopus
Gallus
Mus
Equus
Human-201
Human SERINC5
SERINC2
B)
Vector
Nef
Foamy env
Vector
Coelacanth SERINC2
Xenopus SERINC2
Gallus SERINC2
Mus SERINC2
Equus SERINC2
Human SERINC2
Human SERINC5
C)
Vector (No Nef)
Clade C Nef (HIV-1)
Lai Clade B Nef (HIV-1)
MAC239 Nef (SIV)
Infectivity(%)
150
100
50
0
Vector
Coelacanth
Xenopus
Human
Human SERINC5
SERINC2
D)
Vector
Coelacanth SERINC2
Human SERINC2
Human SERINC5
Relative infectivity (%)
150
100
50
0
HXB2
JRFL
ZM109F
CAP210
VSV-G
E)

Figure 4

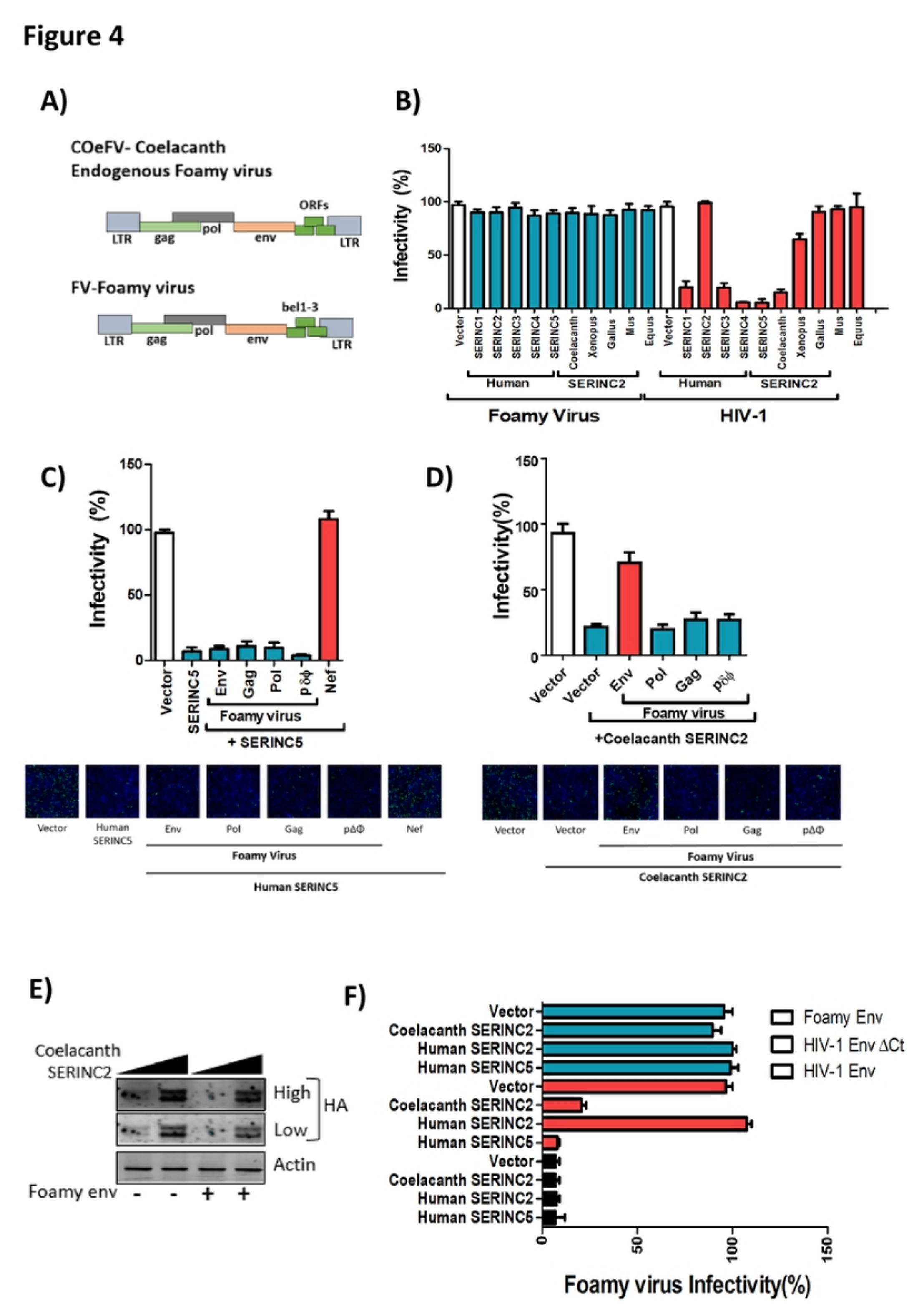
A)
COeFV- Coelacanth
Endogenous Foamy virus
ORFs
LTR
gag
pol
env
LTR
FV-Foamy virus
bel1-3
LTR
gag
pol
env
LTR
B)
Infectivity (%)
150
100
50
0
Vector
SERINC1
SERINC2
SERINC3
SERINC4
SERINC5
Coelacanth
Xenopus
Gallus
Mus
Equus
Human
SERINC2
Foamy Virus
HIV-1
C)
Infectivity (%)
Vector
SERINC5
Env
Gag
Pol
pδϕ
Nef
Foamy virus
+ SERINC5
Vector
Human SERINC5
Env
Pol
Gag
pΔΦ
Nef
Foamy Virus
Human SERINC5
D)
Infectivity(%)
Vector
Vector
Env
Pol
Gag
pδϕ
Foamy virus
+Coelacanth SERINC2
Vector
Vector
Env
Pol
Gag
pΔΦ
Foamy Virus
Coelacanth SERINC2
E)
Coelacanth
SERINC2
High
Low
HA
Actin
Foamy env - - + +
F)
Vector
Coelacanth SERINC2
Human SERINC2
Human SERINC5
Vector
Coelacanth SERINC2
Human SERINC2
Human SERINC5
Vector
Coelacanth SERINC2
Human SERINC2
Human SERINC5
Foamy Env
HIV-1 Env ΔCt
HIV-1 Env
0
50
100
150
Foamy virus Infectivity(%)

Figure 5

A

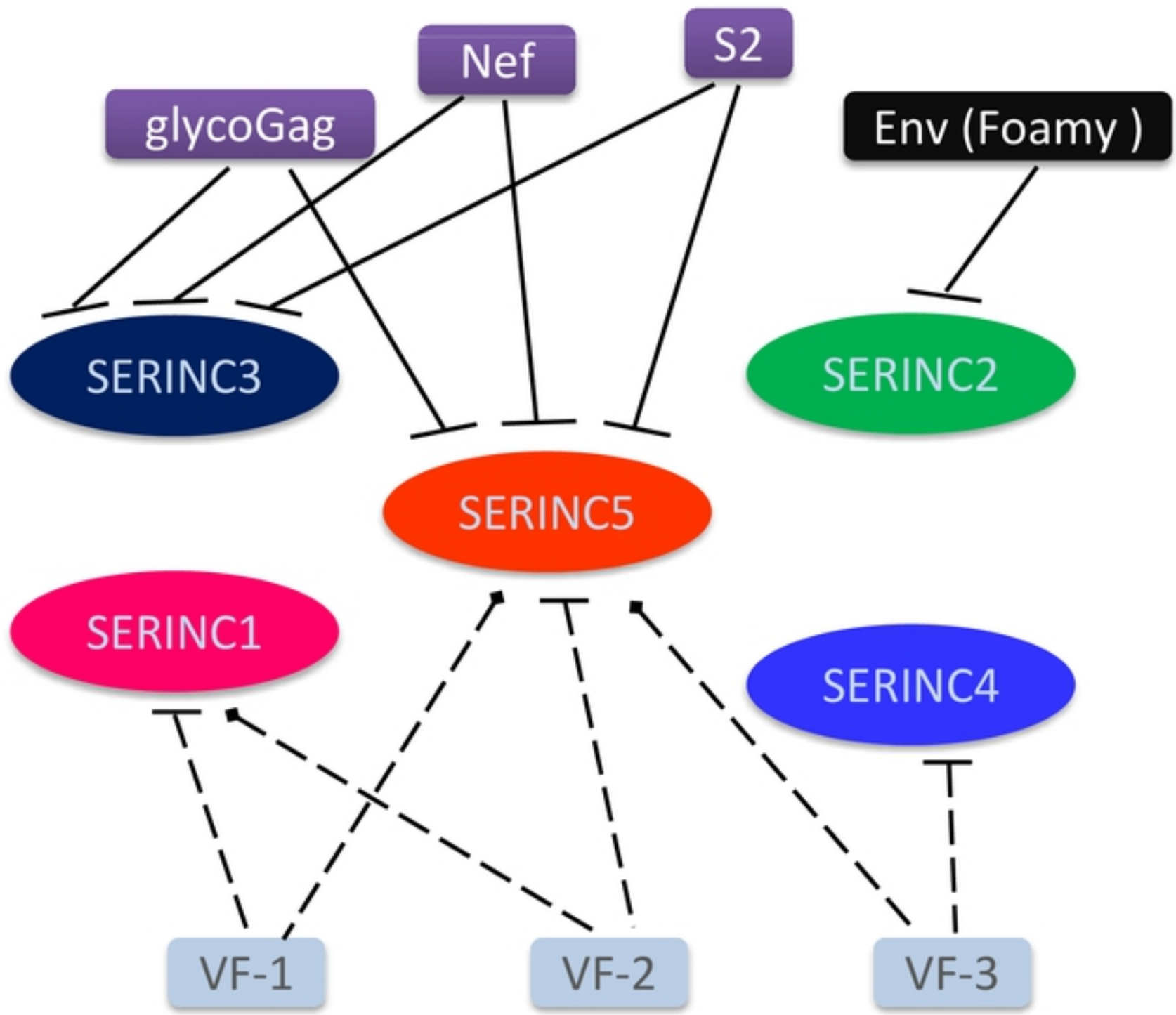
Nef
S2
glycoGag
Env (Foamy)
SERINC3
SERINC2
SERINC5
SERINC1
SERINC4
VF-1
VF-2
VF-3

B

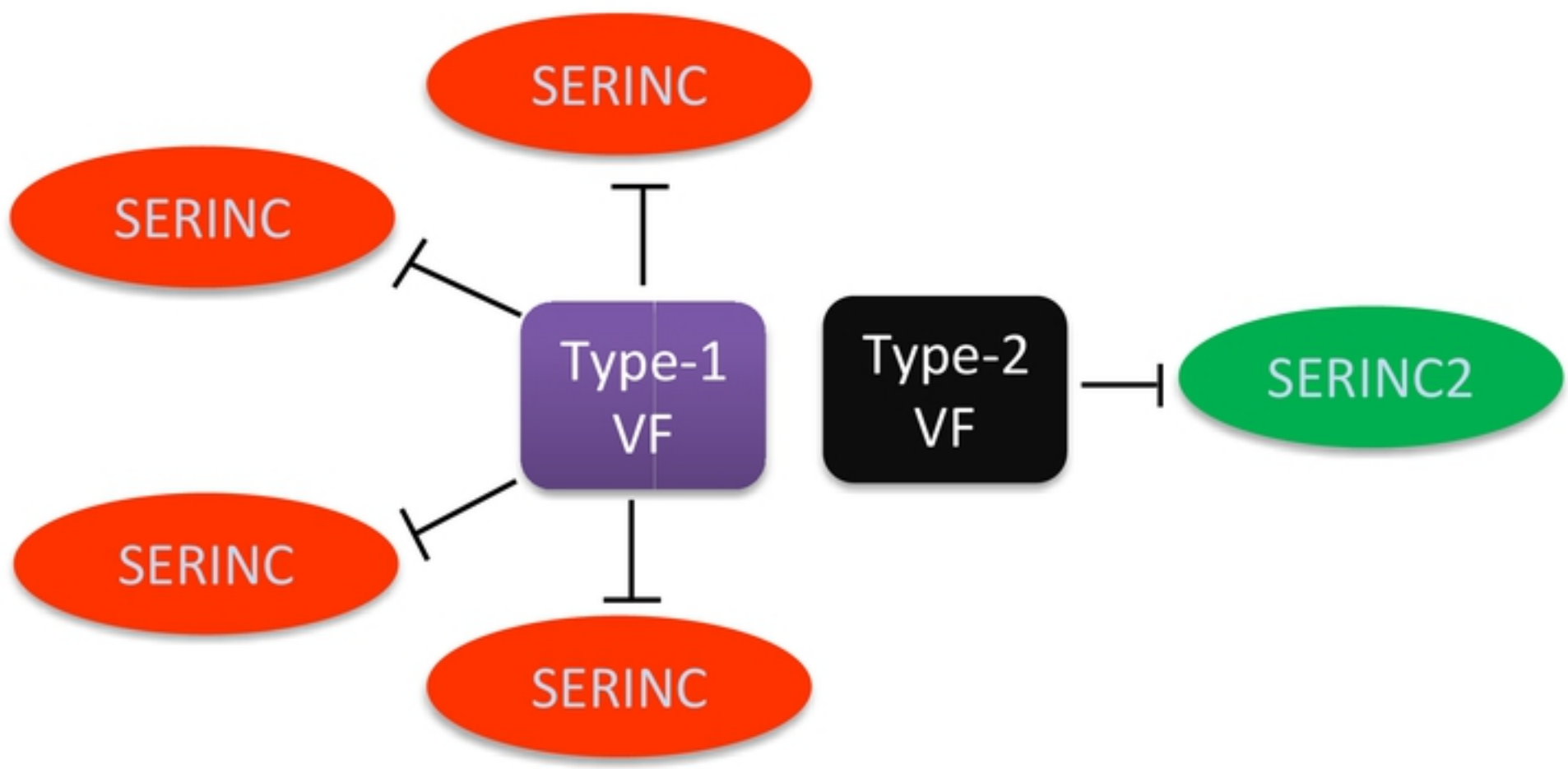
SERINC
SERINC
Type-1
VF
Type-2
VF
SERINC2
SERINC
SERINC